Microscopic analysis of polymerization dynamics with individual actin filaments

Ikuko Fujiwara*, Shin Takahashi*, Hisashi Tadakuma*, Takashi Funatsu* and Shin'ichi Ishiwata*†‡

**Department of Physics, School of Science and Engineering, and †Advanced Research Institute for Science and Engineering, Waseda University, 3-4-1 Okubo, Shinjuku-ku, Tokyo 169-8555, Japan*
‡e-mail: ishiwata@waseda.jp

Published online: 19 August 2002; DOI:10.1038/ncb841

The polymerization–depolymerization dynamics of actin is a key process in a variety of cellular functions. Many spectroscopic studies have been performed in solution, but studies on single actin filaments have just begun. Here, we show that the time course of polymerization of individual filaments consists of a polymerization phase and a subsequent steady-state phase. During the steady-state phase, a treadmilling process of elongation at the barbed end and shortening at the pointed end occurs, in which both components of the process proceed at approximately the same rate. The time correlation of length fluctuation of the filaments in the steady-state phase showed that the polymerization–depolymerization dynamics follow a diffusion (stochastic) process, which cannot be explained by simple association and dissociation of monomers at both ends of the filaments.

To date, there have been many physico-chemical studies of actin polymerization, all of which have been performed in solution. These studies have demonstrated that the polymerization of actin consists of nucleation and growth followed by a steady-state phase, where fragmentation and annealing of filaments may also occur. The average kinetics and thermodynamics of the overall process, and essential elements of these processes, have been experimentally clarified and theoretically formulated[1,2]. Electron microscopy showed that in common with microtubules, actin filaments have a structural polarity, such that the kinetics of polymerization and depolymerization at the two ends of the filaments are different[2–6]. The end of the filaments at which the polymerization rate is higher is called the 'barbed end'. The other end is referred to as the 'pointed end'.

After steady-state polymerization is attained, a treadmilling process is thought to occur[7]. Filament assembly occurs at the barbed end of filaments, whereas depolymerization occurs at the pointed end. This process ensures that the filament maintains a constant average length. The treadmilling process has been examined experimentally in solution[7,8].

When the rate of polymerization is greater than the rate of ATP hydrolysis, ATP-bound actin molecules should cap the ends of the filaments[8]. Depending on whether each end of the actin filaments is capped by ATP-bound actin (ATP cap) or ADP-bound actin (ADP cap), the dynamics of the filaments are predicted to be different, resulting in so-called 'dynamic instability' under appropriate conditions[8,9]. However, in contrast to microtubules[10,11], such a dynamic instability has not yet been demonstrated experimentally with actin filaments. Thus, the examination of whether such a dynamic process occurs with actin is still a challenging problem.

In the 1980s, it became possible to visualize single actin filaments under the fluorescence microscope through labelling with rhodamine–phalloidin (Rh–Ph)[12] or by directly labelling actin with a fluorescent dye, fluorescein isothiocyanate (FITC), and stabilizing the filament with phalloidin[13]. Phalloidin is added to suppress the depolymerization of actin filaments so that they can be imaged at extremely low actin concentrations. This technique is very useful for stable and clear visualization of filaments under a conventional fluorescence microscope, without disturbance of background fluorescence[14,15]. Using this technique, we have previously examined the polymerization process of single actin filaments[16].

In the present study, we have used actin directly labelled with a fluorescent dye. This overcomes the disadvantage of using phalloidin, which suppresses depolymerization. In addition, we have used total internal reflection fluorescence microscopy, which enabled us to study not only the polymerization process, but also the depolymerization process of individual actin filaments under standard polymerization conditions. This technique was recently applied to a study on the polymerization process of single actin filaments in the presence of the Arp2/3 complex[17,18]. Here, not only do we demonstrate the treadmilling process on single actin filaments, but we also extend previous studies by identifying new aspects of the polymerization–depolymerization dynamics of actin.

Results

Direct observation of the polymerization process of single actin filaments. Figure 1 shows direct observation of the actin(Ca) polymerization process, which was induced by the addition of polymerization buffer (potassium chloride and magnesium chloride). Although all the filaments examined were still short at 6 min after the addition of salts (Fig. 1a), most had elongated by more than 10 μm and the total number of filaments had increased after a further 34 min (Fig. 1b). It is clear that most of the filaments grew gradually with time (Fig. 1c–q). Transverse Brownian movement of actin filaments was suppressed by addition of methylcellulose, although longitudinal Brownian movement was not. It seems that there are two types of filament: those that elongated significantly (Fig. 1, white arrows) and those that did not (Fig. 1, arrowheads).

For the initial 30 min of observation, approximately 12% of the filaments showed no elongation (0.7 μM G-actin(Ca); $n = 212$). This may be attributed to adhesion of (or interference with) the filament ends to the glass surface and/or entanglement with methylcellulose, as the proportion of actin filaments that did not elongate detectably was not as high in our previous experiments with Rh–Ph[16], in which methylcellulose was not included.

Next, we examined the time course of change in the total length of individual actin filaments after the addition of salts at 0.3 μM (Fig. 2a), 0.5 μM (Fig. 2b) and 0.7 μM (Fig. 2c) actin. It is clear that the polymerization process of each filament consists of a polymerization phase and a subsequent steady-state phase (Fig. 2c). These two phases were not easily distinguishable at lower actin concentrations.

Table 1 **Polymerization and depolymerization rate constants.**

Conditions		k^+ (M^{-1} s^{-1})	k^- (s^{-1})	C_0 (μM)
		$\times 10^7$		
Steady-state phase*	Ca	18	25	—
	Mg	45	29	—
Polymerization phase†	Ca	0.61	0.85	0.14
	Mg	1.0	0.64	0.064
Solution + 0.5%	Ca	0.75	0.94	0.13
methylcellulose‡	Mg	1.2	0.80	0.067
Solution§	Ca	0.50	0.57	0.11
	Mg	0.95	0.90	0.095

Conditions: 30 mM potassium chloride, 2 mM magnesium chloride, 4 mM ATP, 20 mM MOPS at pH 7.0, 10 mM DTT, with*†‡ or without§ 0.5% (w/v) methylcellulose.

*Estimated from the analysis of length fluctuation in the steady-state phase in single-molecule analysis.

†Estimated from the average length change in the polymerization phase in single-molecule analysis.

‡,§Obtained from the initial rate of increase in the fluorescence intensity in solution in the presence‡ or absence§ of methylcellulose.

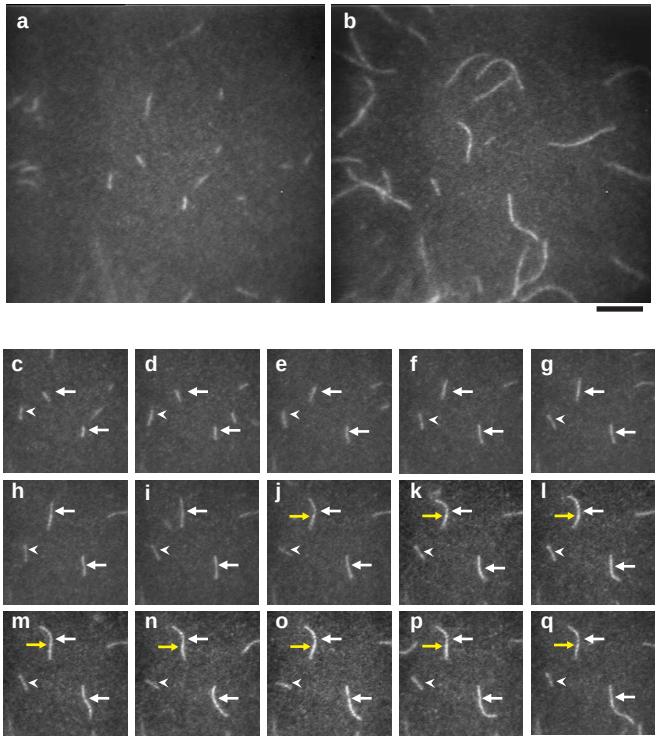

Figure 1 **Fluorescence micrographs of actin(Ca) polymerization. a**,**b**, Fluorescence micrographs taken 6 min (**a**) and 34 min (**b**) after the addition of salts (movies are available at http://www.phys.waseda.ac.jp/bio/ishiwata/movies.html). **c**–**q**, Fluorescence micrographs of the central regions in **a** and **b**, in which several filaments were visualized without interference by overlapping filaments. Micrographs were taken every 2 min, between 6 min (**c**) and 34 min (**q**) after the addition of salts. White arrows indicate the filaments for which polymerization could be observed, whereas an arrowhead indicates a filament which did not seem to polymerize. Yellow arrows indicate an example of a fluorescent blob on the actin filament, which was used as a fiducial marker to measure the length change at each end of the filament. Actin concentration, 0.7 μM. Scale bar represents 10 μm.

It is notable, especially in Fig. 2c, that the time at which the steady-state phase began varied between filaments. In both phases, all the actin filaments displayed small fluctuations in length. We did not observe any filaments that only underwent depolymerization or displayed any dynamic instability[10,11], as previously observed for microtubules. Occasionally, a large change in length, as a result of head-to-tail annealing of two filaments[4] (longer than a few microns), was observed. However, these data were not used for the analysis described below, as we focused on the polymerization–depolymerization dynamics at both ends of the filaments. We did not observe spontaneous fragmentation of actin filaments, as observed in the presence of gelsolin[16].

Generally, a fluorescence image of an actin filament (that is, an intensity profile along the filament) is not uniform. Indeed, we detected fluorescent blobs at fixed positions on the filaments (Fig. 1, yellow arrows). Using a blob as a fiducial marker, we measured the length of the filament portions on each side of the fluorescent marker (Fig. 2d). These measurements show that after the steady-state phase was attained, the filament continued growing at one end, whereas it began to shorten correspondingly at the other end. We assign the former as the barbed end and the latter as the pointed end, on the basis of the known difference in critical concentration for the two ends of the filament. This result demonstrates that the treadmilling process can occur on an individual actin filament. Among the data at 0.7 μM actin(Ca), we found seven examples that had a bright marker sufficient for quantitative analysis of the polymerization process at each end of the filament. At the steady-state phase, the polymerization rate averaged over these seven cases was $+0.069 \pm 0.037$ μm min^{-1} (± standard deviation, S.D.) at the fast-growing end (barbed end), -0.062 ± 0.051 μm min^{-1} at the slow-growing end (pointed end) and 0.006 ± 0.062 μm min^{-1} for the total length of the filaments. This confirms that on average, the growing rate at the barbed end was compensated by the shortening rate at the pointed end. However, the growing and the shortening rates did not necessarily coincide with each other in each filament, at least within the time range we examined (8–30 min).

As a control, the time course of length change in a single actin filament at steady state in the presence of phalloidin was determined (Fig. 2e). Phalloidin was added to a final concentration of 150 nM, which is equal to the actin concentration and higher than the dissociation constant of phalloidin to actin (17 nM)[19].

Estimation of the polymerization rate of actin(Ca) during the polymerization phase. To determine the relationship between the polymerization rate and actin concentration, we analysed the change in length of actin filaments for 6 min after commencing microscopic observation. This represents the polymerization rate of actin during the initial polymerization phase (Fig. 2). We failed to record the earliest initial phase of polymerization; however, the polymerization rate estimated from our measurements is reliable, as linear extrapolation of our data passes through the origin (zero length at time zero).

The change in length was measured at 1-min intervals for the initial 6-min observation period (Fig. 2). The data is presented as a histogram, showing the distribution of the change in length at three different concentrations of actin (Fig. 3a–c). Thus, the polymerization rate obtained from the average distribution and the S.D. from the width of the distribution are estimated as 0.13 ± 0.30 μm min^{-1}, 0.35 ± 0.38 μm min^{-1} and 0.49 ± 0.46 μm min^{-1} at 0.3, 0.5 and 0.7 μM actin, respectively. The relationship between the polymerization rate and the actin concentration is summarized in Fig. 3d. On the basis that an actin filament of 1 μm in length consists of 400 monomers, polymerization and depolymerization rate constants were estimated to be 6.1×10^6 M^{-1} s^{-1} and 0.85 s^{-1}, respectively. The critical concentration for polymerization was determined as 0.14 μM (see Table 1).

Analysis of length fluctuation of actin(Ca). The total length of

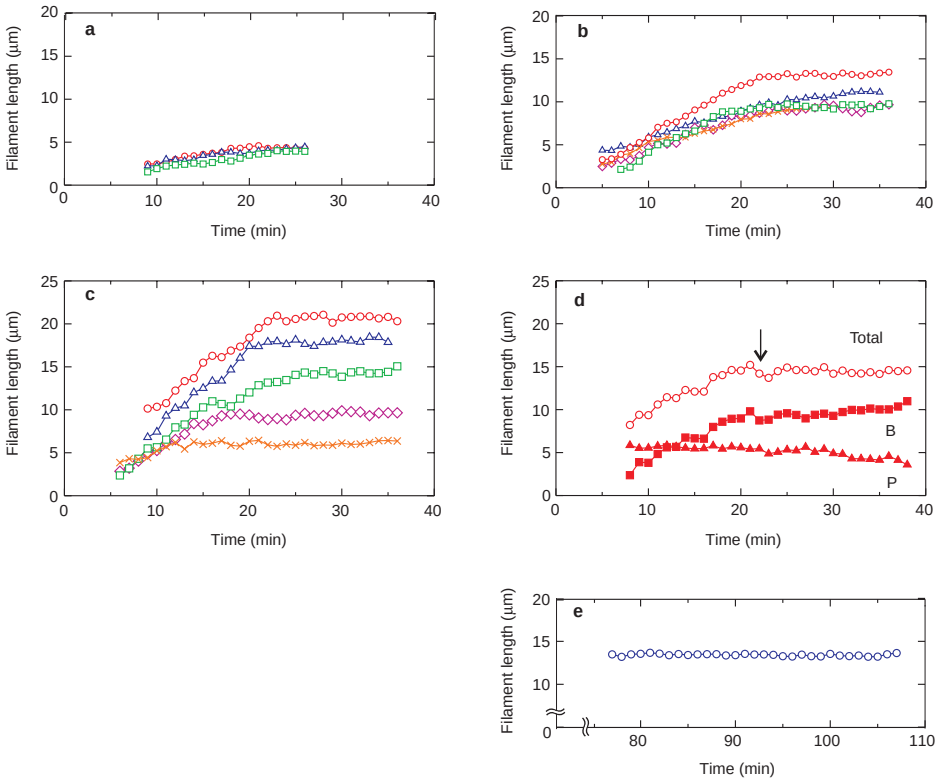

Figure 2 **Time course of actin(Ca) polymerization at various actin concentrations. a–c**, Examples showing the time course of polymerization of single actin(Ca) filaments at 0.3 μM (**a**), 0.5 μM (**b**) and 0.7 μM (**c**) actin. **d**, An example showing the time course of polymerization of a single actin(Ca) filament (actin, 0.7 μM), in which the barbed end and pointed end could be distinguished. An arrow indicates the start of the steady-state phase. Total, total length of the actin filament; B, length between the barbed end and the fluorescent marker; P, length between the pointed end and the fluorescent marker. **e**, A control time course experiment showing the length fluctuation of actin(Ca) filaments stabilized with phalloidin. To maintain the same conditions that were used for the above experiments without phallotoxin, the proportion of TMR-labelled actin was adjusted to 10% of total. Additionally, G-actin(Ca) was added to a final concentration of 140 nM, a critical concentration for polymerization (see Table 1), to match the background fluorescence noise of samples without phallotoxin (see Discussion). Here, the filament length was measured between 77 and 107 min after the observation cell was prepared. Actin and phalloidin were used at 0.15 μM.

each actin filament fluctuated continuously with time (Fig. 2). Fluctuations not only occurred during the polymerization phase (where the length of the filaments increased steadily), but also during the steady-state phase (where the average length of the filaments was almost constant). To examine whether this fluctuation in length could also provide information on the dynamics of polymerization–depolymerization, we analysed the relationship between time and the fluctuation of length. The change in length during various time intervals, termed the correlation time, τ, was measured in the steady-state phase (Fig. 4a). If the fluctuations in length are caused solely by random error in the measurements, then they should be independent of τ.

To confirm the above hypothesis, we examined the effect of phallotoxin, which is expected to suppress the length change caused by depolymerization. In fact, the addition of phalloidin significantly reduced the fluctuation in length (Fig. 2e). Furthermore, as expected, the width of the distribution of length fluctuation seemed to be almost independent of τ (Fig. 4b). This suggests that the width of the distribution obtained for the phallotoxin-labelled actin filaments may represent the degree of error in the length measurements.

By contrast, the width of the distribution of length fluctuation obtained for actin filaments without phallotoxin increased coordinately with τ, whereas the average of the distribution was almost zero, implying that the steady-state phase had been attained (Fig. 4c).

Polymerization dynamics of actin(Mg). The same polymerization properties described above for actin(Ca) have also been shown for actin(Mg)[20]. In contrast to actin(Ca), the resolution of length measurements was lower because of the lower contrast of the fluorescence image. This is probably attributable to a large background fluorescence originating from a large number of short filaments, because nucleation occurs more easily with actin(Mg).

Fluorescence images of polymerized filaments taken 7 and 35 min after the addition of salts showed that the filament density seems to be higher than that of actin(Ca), even if the actin concentration was less than half (compare Fig. 5a with Fig. 1). Furthermore, the polymerization rate constant was 1.0×10^7 $M^{-1}s^{-1}$, approximately twice that of actin(Ca), and the depolymerization rate constant was 0.6 s^{-1} (Fig. 5b). The critical concentration was 0.064 μM (see Table 1).

Next, we analysed the length fluctuation of actin(Mg) filaments once the steady-state phase had been achieved (Fig. 5c). As observed in Fig 5c,d, the degree of length fluctuation of actin(Mg) was larger than that of actin(Ca) (note that the width (S.D.) of the distribution in Fig. 5d is greater than that in Fig. 4c).

Polymerization dynamics of single actin filaments follow a diffusion process. We examined the polymerization and depolymerization dynamics of single actin filaments by analysing the distribution of the length fluctuation during the steady-state phase (Figs 4c,5d). If the fluctuation in length is a result of errors in measurement, it must be independent of τ. However, if it originates from the stochastic process of actin polymerization and depolymerization at both ends of the filaments, the square of the distribution width (S.D.) must be proportional to τ (see ref. 21, chapter 4) and its analysis will provide information on the polymerization–depolymerization dynamics, as described below. To examine this mechanism, we obtained a relationship between $(S.D.)^2$ and τ, as shown in Fig. 6. As a control, we

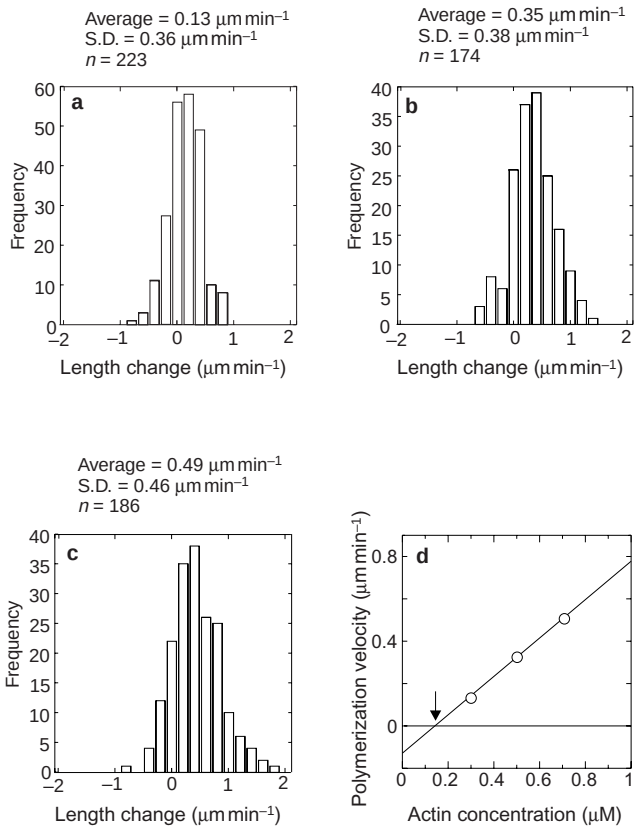

Figure 3 **The effects of G-actin(Ca) concentration on filament growth during polymerization.** The rate of change in length for actin filaments in the polymerization phase is shown for 0.3 μM (**a**), 0.5 μM (**b**) and 0.7 μM (**c**) G-actin(Ca). Data were collected for 6 min after the time at which the length measurement could be initiated (see Fig. 2a–c). The histograms show not only the magnitude of the length fluctuation during polymerization (from the S.D. of the histogram), but also the average polymerization rate (from the centre of the histogram). The average polymerization velocity, the width of the histogram and the total number of measurements (*n*) are shown. **d**, The relationship between the average polymerization rate and actin concentration. The arrow indicates the critical actin concentration for polymerization. The slope indicates the polymerization rate and the intercept of this line with the *y* axis indicates an apparent depolymerization rate.

obtained the same relationship for the phallotoxin-labelled actin filaments under different levels of background fluorescence noise (Fig. 6a).

The line describing the relationship between $(S.D.)^2$ and τ did not pass through the origin, but intersected with the *y* axis for both kinds of actin (Ca or Mg). Thus, the relationship between $(S.D.)^2$ and τ could be expressed as $(S.D.)^2 = (S.D._0)^2 + \alpha\tau$, where α is a constant. We considered that the constant term, $(S.D._0)^2$, is attributable to a measurement error caused by the spatial resolution, which depends on the contrast of the fluorescence image of actin filaments.

It is understandable that the $S.D._0$ value of phallotoxin-labelled actin filaments was smaller (Figs 4b,6a) if we consider that the contrast of the fluorescence image was much higher. To ensure the validity of this explanation, we examined the length fluctuation of phallotoxin-labelled actin filaments at different levels of background fluorescence noise by adding 10%-labelled (Fig. 6a, open triangles and squares) or 50%-labelled (Fig. 6a, closed triangles) G-actin(Ca). We confirmed that the value of $S.D._0$ increased as the contrast of filament fluorescence image decreased (through an increase in the background fluorescence noise). Thus, we conclude that the reason why the value of $S.D._0$ for actin(Mg) (Fig. 6b) was larger than that for actin(Ca) (Fig. 6a) is that the contrast of fluorescence image of actin(Mg) filaments was worse than that of actin(Ca).

Discussion

Treadmilling of actin filaments was first introduced as a theory by Wegner[7] in 1976. Since then, the process has been studied extensively, although only in solutions containing many actin filaments. Here, we have shown through direct examination that the treadmilling process also occurs at the level of individual actin filaments. We observed that continuous elongation at the barbed end and shortening at the pointed end occurred on individual actin filaments during the steady-state phase (Fig. 2d). We also demonstrated that dynamic instability, as observed in microtubules[10,11], does not occur, at least in pure actin filaments.

Here, we formulate the theoretical basis for the linear relationship between $(S.D.)^2$ and τ obtained by analysis of the length fluctuation (Fig. 6)[21]. Assuming that the length fluctuation of actin filaments is caused by the stochastic process of association and dissociation of actin, the existence probability of actin filaments of length x, at time t, $P(x,t)$, $(0 \le P(x,t) \le 1)$, is determined by the following differential equation,

$$\frac{\partial P(x,t)}{\partial t} = \{k^- P(x+a) - k^+ CP(x)\} + \{k^+ CP(x-a) - k^- P(x)\} \quad (1)$$

where k^+ and k^- are a polymerization and a depolymerization rate constant, respectively, C is the concentration of the polymerization unit (in the simplest case, actin monomers) coexisting with the filaments, and a is an effective length of polymerization and depolymerization unit (in the simplest case, a represents an effective length of an actin subunit in the filament, that is, 2.7 nm). When we distinguish the barbed end and the pointed end, $k^+ = k_B^+ + k_P^+$ and $k^- = k_B^- + k_P^-$, where $k_{B(P)}^+$ and $k_{B(P)}^-$ are the polymerization and depolymerization rates at the B(P)-end, respectively. Also, note that the present model does not explicitly take into account the heterogeneous state of actin subunits in the filaments coupled with ATP hydrolysis (see below).

Equation 1 is reduced to equation 2 (see below), which is the equivalent of a diffusion equation. Here, we expand the $P(x+a)$ and $P(x-a)$ terms in equation 1 with the Taylor series at x, assuming $a << x$ and remain the first three terms up to those containing a^2.

$$\frac{\partial P(x,t)}{\partial t} = \frac{1}{2} a^2 \frac{\partial^2 P(x,t)}{\partial x^2} (k^+C + k^-) - a^2 \frac{\partial P(x,t)}{\partial x} (k^+C - k^-) \quad (2)$$

The first term and the second term in the right side of the equation are attributed to diffusion and net polymerization (flow term), respectively. The proportionality coefficient in the first term corresponds to the diffusion coefficient D, which appears in the diffusion equation, as

$$D = \frac{1}{2} a^2 (k^+C + k^-) \quad (3)$$

Note that C in the steady-state phase must be C_0, that is, the critical concentration for polymerization of actin when the polymerization unit is an actin monomer.

The fact that $(S.D.)^2$ was proportional to τ (Fig. 6) demonstrates that the polymerization–depolymerization dynamics at both ends

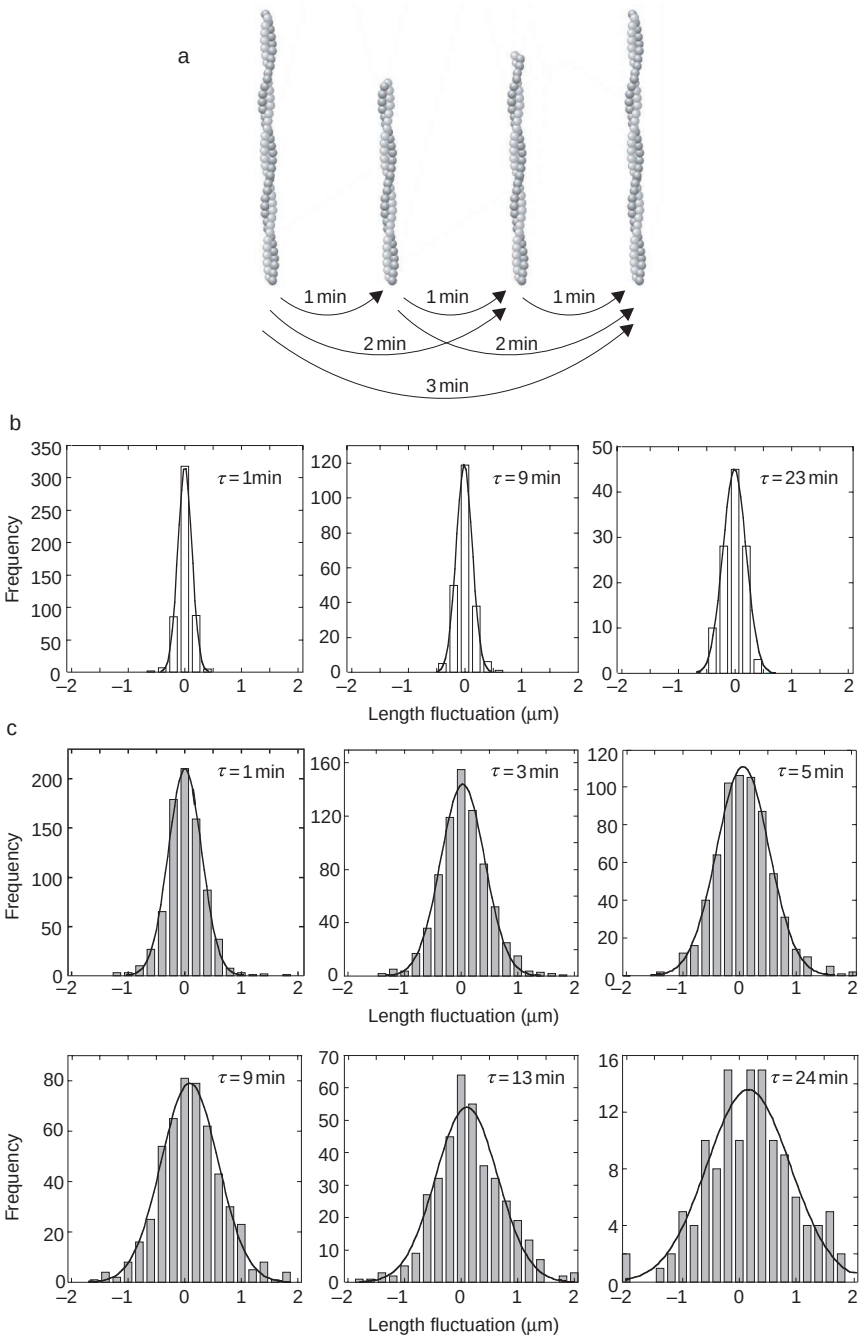

Figure 4 **Frequency of actin(Ca) filament length fluctuation in a steady-state phase. a**, A schematic illustration of how to measure the frequency of length fluctuation. The change in the length of filaments was measured at intervals of τ min, as indicated. **b**,**c**, Histograms showing the frequency of length fluctuations at various values of τ in the presence (**b**) or absence (**c**) of phalloidin (0.15 μM). Note that the average polymerization velocity was almost zero, independent of the value of τ, implying that a steady-state phase had been attained. Actin was used at 0.15 μM (**b**) or 0.7 μM (**c**).

of actin filaments obey the diffusion (stochastic) process, such that $(\text{S.D.})^2 = 2D\tau = a^2(k^+C_0 + k^-)\tau$. This is because we have confirmed that the steady-state phase has been attained, so that the flow term in the right side of equation 2 can be neglected ($k^+C = k^-$ at $C = C_0$). Thus, we can estimate the kinetic constants for polymerization and depolymerization during the steady-state phase from the slope of the relationship shown in Fig. 6. The slight positive slope of the $(\text{S.D.})^2$ versus τ relationship observed in the phallotoxin-labelled filaments (Fig. 6a) is attributable to a gradual lowering of the fluorescence contrast of the image through photo-bleaching. Thus, the large slope observed in the absence of phallotoxin may include this effect, but it is negligible.

To obtain the polymerization and depolymerization rate constants during the steady-state phase, the values of C_0 obtained above, 0.14 μM for actin(Ca) and 0.064 μM for actin(Mg) (Figs 3d,5b) were used. Assuming that the value of a is 2.7 nm, the values of k^+ and k^- have been estimated as 1.8×10^8 $M^{-1}s^{-1}$ and 25 s^{-1} for actin(Ca) (Fig. 6a) and 4.5×10^8 $M^{-1}s^{-1}$ and 29 s^{-1} for actin(Mg) (Fig. 6b), respectively. Unexpectedly, the values were 30–45 times larger than those obtained from the polymerization phase. The results of our analysis are summarized in Table 1 and a possible reason for such a discrepancy is discussed below.

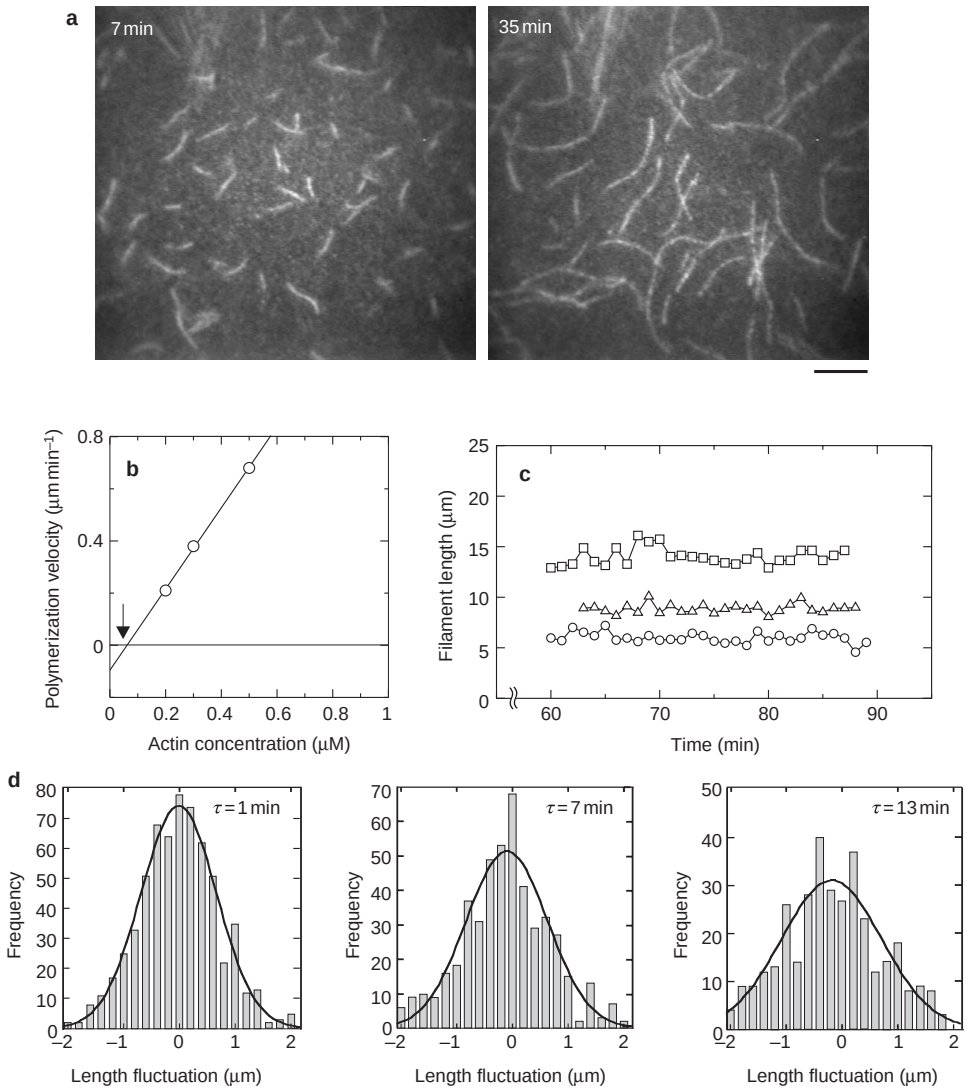

Figure 5 **Analysis of the polymerization dynamics of actin(Mg).** **a**, Fluorescence micrographs show polymerized filaments 7 min and 35 min after the addition of salts. Scale bar represents 10 μm. **b**, The relationship between average polymerization velocity and actin concentration. The arrow indicates the critical actin concentration for polymerization (see Fig. 3d). The slope of the linear approximation line shows the polymerization rate and the intercept of this line with the *y* axis indicates an apparent depolymerization rate. **c**, Three examples showing the length fluctuation observed at steady state. Actin was used at 0.3 μM in **a** and **c**. **d**, Histograms showing the frequency of length change at several values of τ.

In conclusion, we will summarize the polymerization and depolymerization rates and the critical concentration for polymerization obtained through different methods. As shown in Table 1, the kinetic constants were consistent, except for those estimated from the analysis of the length fluctuation at steady state on the basis of the diffusion process. The latter was approximately 40 times larger than the others. Also, note that the critical concentration for actin(Ca) obtained in the present study was smaller than that for actin(Ca) in which polymerization was induced by calcium[6]. This is probably because in our experiments, calcium attached to actin(Ca) monomers can exchange with free magnesium after the addition of salts (potassium chloride and magnesium chloride), so that actin(Ca) may have partly been transformed into actin(Mg).

There are several possible reasons for the apparent discrepancy between the kinetic constants described above: first, the kinetic constants obtained in the steady-state phase may be intrinsically different from those obtained in the initial phase of polymerization. As previously reported[9], the ratio of ADP-type to ATP-type actin at both ends of the filaments is larger in the steady-state phase than in the initial phase of polymerization. It is known that the depolymerization velocity of ADP-actin is an order of magnitude higher than that of ATP-actin, at least at the barbed end[6]. Second, the annealing of actin fragments may be responsible, as for the large polymerization rate that must be balanced by the depolymerization rate in the steady-state phase. As previously reported, the annealing rate constant is comparable to the polymerization rate (10^7 $M^{-1}s^{-1}$, ref. 22; for qualitative data, see ref. 4). This suggests that a polymerization unit may not be a monomer alone, but an average of monomers, oligomers and fragments. In addition, the size of the depolymerization unit may be different from that of the polymerization unit described above. Third, the size of a polymerization–depolymerization unit, *a*, may not necessarily indicate a size of a monomer, an oligomer and a fragment of actin, as described above. Rather, it may represent an effective size of a unit involved in cooperative (consecutive) polymerization and depolymerization, implying that each cycle of polymerization and depolymerization is

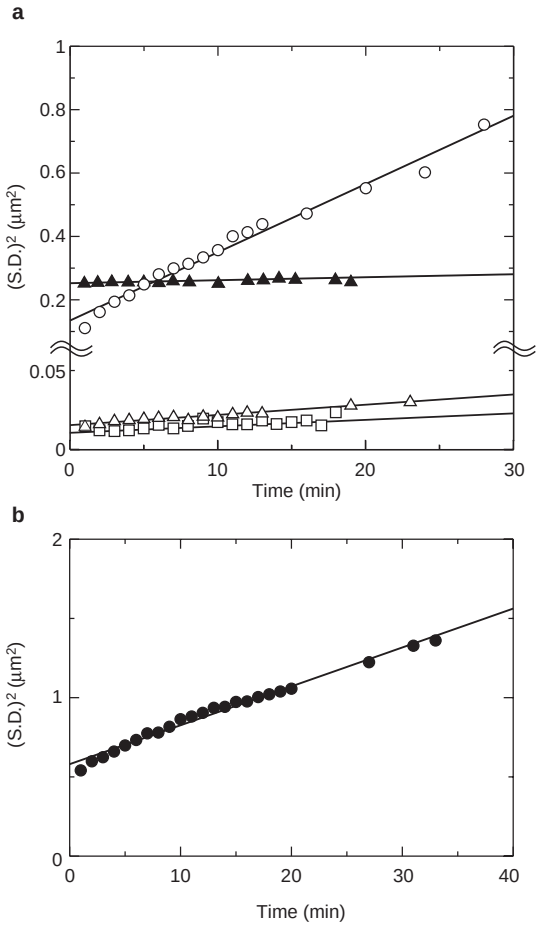

Figure 6 **Square of the width of the length fluctuation histogram versus correlation time.** This relationship was obtained at steady state (Figs 4,5). **a**, Actin (Ca). Circles represent 0.7 μM actin(Ca) without phallotoxin (see Fig. 4c), where $(S.D.)^2 = 0.022\tau + 0.14$. Open and closed triangles represent 0.15 μM phalloidin–actin(Ca), where $(S.D.)^2 = 0.00065\tau + 0.016$ for open triangles (see Fig. 4b) and $(S.D.)^2 = 0.00071\tau + 0.25$ for closed triangles. After actin filaments were stabilized with phalloidin, 0.14 μM G-actin(Ca), of which 10% (open triangles) or 50% (closed triangles) was TMR-labelled, was added to produce a fluorescence background noise. Open squares represent 0.15 μM phallacidin–actin(Ca), where $(S.D.)^2 = 0.00041\tau + 0.015$. As above, 0.14 μM G-actin(Ca), of which 10% was TMR-labelled, was added. **b**, 0.3 μM actin(Mg) without phallotoxin (see Fig. 5d), where $(S.D.)^2 = 0.025\tau + 0.58$.

dependent on the previous one (a non-Markov process). In fact, the treadmilling (cooperative) process occurs through the coupling of polymerization with ATP hydrolysis on actin, which may be equivalent to dynamic instability for actin. Whatever the mechanism, one plausible way to account for the large (40×) rate constants is through a difference in the effective size of *a*. If *a* is approximately six times larger than that of actin monomers, using equation 3, a^2 becomes 36 times larger, which is a close approximation of the 40× values. To clarify the polymerization–depolymerization dynamics at each end of the filaments, we need more detailed analysis of length change, with higher spatio-temporal resolution after distinguishing the barbed end and the pointed end.

Significantly, the usual methods used to monitor the average process of polymerization and depolymerization may miss the annealing process discussed above. For example, the fluorescence intensity of pyrene is very sensitive to the polymerization and depolymerization of monomers, but insensitive to the annealing of fragments. This may explain why, on the basis of analysis of incorporation of pyrene-labelled actin into the filaments in the steady-state phase, Brenner and Korn[23] obtained the kinetic constants consistent with those obtained from the polymerization phase, but did not find a discrepancy similar to that found in this study.

Thus, the single-filament analysis of actin polymerization has not only demonstrated the treadmilling process on single actin filaments, but has also identified a new aspect of polymerization–depolymerization dynamics by making it possible to analyse fluctuations in length at steady state. The present results indicate that the polymerization–depolymerization dynamics of pure actin filaments are not as 'dynamic' as those of microtubules. However, because actin is a central component of the cytoskeleton, a wide variety of actin-specific dynamic processes exist. It will be important to investigate the effects of various actin-binding proteins on the polymerization phase and the length fluctuations of actin filaments at steady state. We infer that the dynamic properties of polymerization and depolymerization of pure filaments may allow actin to perform different dynamic functions in different cell types, through interactions with cell-specific regulatory proteins. □

Methods

Preparation of actin

G-actin(Ca) was prepared from rabbit muscle according to Spudich and Watt[24], except that the tropomyosin–troponin complex was removed before preparing acetone powder, as previously desctibed[4]. G-actin(Ca) was solubilized in 2 mM Tris-HCl at pH 8.0, 0.1 mM calcium chloride, 0.1 mM ATP (Boehringer Ingelheim, Ingelheim, Germany) and 2 mM sodium azide. The concentration of actin was determined from ultraviolet absorption (UV 2000, Shimadzu, Japan) with $A^{1\%}_{290} = 6.3\ cm^{-1}$.

Labelling of actin with fluorescent dye was performed by incubating 1.7 mg ml^{-1} F-actin in a solution containing 0.1 M potassium chloride, 0.2 mM magnesium chloride, 0.1 mM ATP, 10 mM MOPS at pH 7.0 and 100 μM tetramethylrhodamine-5-maleimide (TMR-5-MA; Molecular Probes, Eugene, OR) dissolved in dimethylformamide (DMF; Sigma, St Louis, MO) for 2 h at room temperature. TMR-5-MA (20 mM) dissolved in DMF was slowly added to the F-actin solution with continuous stirring. TMR-labelled F-actin was centrifuged at 411,000*g* for 45 min at 8 °C. The pellet was then dissolved in and dialysed against 20 mM PIPES at pH 6.8, 0.1 mM ATP and 0.1 mM calcium chloride overnight at 2 °C. After centrifugation at 411,000*g* for 20 min at 2 °C, the fluorescent dye was removed from the G-actin solution by Sephadex G-25 column chromatograpy. The concentration of TMR was estimated from the molar extinction coefficient at 550 nm, 96,900 $M^{-1}cm^{-1}$ (Molecular Probes). The concentration of labelled G-actin(Ca) was determined by subtracting $0.208 \times A_{550}$ from the A_{290} value. The molar ratio of the label to actin was estimated to be >96%. TMR-labelled G-actin(Mg) was prepared by incubating labelled G-actin(Ca) in 0.2 mM EGTA (Dojindo, Kumamoto, Japan), 0.1 mM ATP, 20 mM PIPES at pH 6.8 and 0.1 mM magnesium chloride for 60 min at 0 °C[25] before centrifugation at 350,000*g* for 1 h at 2 °C. The supernatant was used as labelled G-actin(Mg). Pyrenyl–actin was prepared as previously described[26].

Experimental conditions

For microscopic examination, the *in vitro* polymerization of actin was initiated by addition of polymerization buffer (final concentrations: 30 mM potassium chloride, 2 mM magnesium chloride, 4 mM ATP, 20 mM MOPS at pH 7.0, 10 mM dithiothreitol (DTT) and 0.5% (w/v) methylcellulose) at 27 °C. This solution was then immediately transferred to a glass coverslip before microscopic examination. The proportion of TMR-labelled actin was maintained at 10%. It has been confirmed that at this labelling ratio, the polymerization rate and critical concentration in solution are unchanged[18]. For examination in solution, polymerization of actin(Ca or Mg) containing 10% pyrenyl–actin was initiated in a cuvette by adding the polymerization buffer, with or without methylcellulose. Fluorescence intensity was measured at 27 °C in a fluorescence spectrophotometer (F-4500, Hitachi, Tokyo, Japan). We confirmed that methylcellulose does not affect the average polymerization properties of actin in solution (Table 1). When the effect of phallotoxin was examined, the phallotoxin (phalloidin or phallacidin; Sigma) was added after the polymerization of actin(Ca) (10% TMR-labelled) was complete. The length of phallotoxin-labelled actin filaments was measured after a 1:10 dilution of the solution against the polymerization buffer containing 0.14 μM G-actin(Ca) (the critical concentration for polymerization), of which either 10% or 50% was labelled with TMR as background fluorescence noise. Here, we examined not only phalloidin, but also phallacidin, because the stabilizing properties of phallacidin for actin filaments seemed to be stronger than those of phalloidin (see ref. 16).

Optical system

Fluorescently labelled single actin filaments were visualized by total internal reflection fluorescence microscopy[27] (IX70, Olympus, Tokyo, Japan), which illuminates to a depth of only ~150nm below the coverslip. Samples were illuminated with a green laser (μ-Green model 4301-050; Uniphase, San Jose, CA). After 100 video frames (duration 3 s) were superimposed by using a digital image processing system (DIPS, Hamamatsu Photonics, Hamamatsu, Japan), the length of actin filaments was measured. The distance between adjacent pixels was 0.128 μm, to which the spatial resolution was limited.

RECEIVED 25 FEBRUARY 2002; REVISED 15 JUNE 2002; ACCEPTED 17 JULY 2002;
PUBLISHED 19 AUGUST 2002.

1. Oosawa, F. & Kasai, M. Theory of linear and helical aggregations of macromolecules. *J. Mol. Biol.* **4,** 12–15 (1962).
2. Oosawa, F. & Asakura, S. *Thermodynamics of the Polymerization of Proteins* (Academic Press, New York, 1975).
3. Woodrum, D. T., Rich, S. A. & Pollard, T. D. Evidence for biased bidirectional polymerization of actin filaments using heavy meromyosin prepared by an improved method. *J. Cell Biol.* **67,** 231–237 (1975).
4. Kondo, H. & Ishiwata, S. Uni-directional growth of F-actin. *J. Biochem.* **79,** 159–171 (1976).
5. Hayashi, T. & Ip, W. Polymerization polarity of actin. *J. Mechanochem. Cell Motil.* **3,** 163–169 (1976).
6. Pollard, T. D. & Cooper, J. A. Actin and actin-binding proteins. A critical evaluation of mechanism and functions. *Annu. Rev. Biochem.* **55,** 987–1035 (1986).
7. Wegner, A. Head to tail polymerization of actin. *J. Mol. Biol.* **108,** 139–150 (1976).
8. Korn, E. D., Carlier, M.-F. & Pantaloni, D. Actin polymerization and ATP hydrolysis. *Science* **238,** 638–644 (1987).
9. Carlier, M.-F. Role of nucleotide hydrolysis in the dynamics of actin filaments and microtubules. *Int. Rev. Cytol.* **115,** 139–170 (1989).
10. Mitchison, T. & Kirschner, M. Dynamic instability of microtubule growth. *Nature* **312,** 237–242 (1984).
11. Horio, T. & Hotani, H. Visualization of the dynamic instability of individual microtubles by dark-field microscopy. *Nature* **321,** 605–607 (1986).
12. Yanagida, T., Nakase, M., Nishiyama, K. & Oosawa, F. Direct observation of motion of single actin filaments in the presence of myosin. *Nature* **307,** 58–60 (1984).
13. Honda, H., Nagashima, H. & Asakura, S. Directional movement of F-actin *in vitro*. *J. Mol. Biol.* **191,** 131–133 (1986).
14. Harada, Y., Sakurada, K., Aoki, T., Thomas, D. D. & Yanagida, T. Mechanochemical coupling in actomyosin energy transduction studied by *in vitro* movement assay. *J. Mol. Biol.* **216,** 49–68 (1991).
15. Huang, Z. J., Haugland, R. P., You, W. M. & Haugland, R. P. Phallotoxin and actin binding assay by fluorescence enhancement. *Anal. Biochem.* **200,** 199–204 (1992).
16. Ishiwata, S., Tadashige, J., Masui, I., Nishizaka, T. & Kinosita, K. Jr in *Molecular Interactions of Actin* (eds dos Remedios, C. G. & Thomas, D. D.) 79–94 (Springer-Verlag, Heidelberg, 2001).
17. Amann, K. J. & Pollard, T. D. Direct real-time observation of actin filament branching mediated by Arp2/3 complex using total internal reflection fluorescence microscopy. *Proc. Natl Acad. Sci. USA* **98,** 15009–15013 (2001).
18. Fujiwara, I., Suetsugu, S., Uemura, S., Takenawa, T. & Ishiwata, S. Visualization and force measurement of branching by Arp2/3 complex and N-WASP in actin filament. *Biochem. Biophys. Res. Comm.* **293,** 1550–1555 (2002).
19. De La Cruz, E. M. & Pollard, T. D. Kinetics and thermodynamics of phalloidin binding to actin filaments from three divergent species. *Biochemistry* **35,** 14054–14061 (1994).
20. Estes, J. E., Selden, L. A., Kinosian, H. J. & Gershman, L. C. Tightly-bound divalent cation of actin. *J. Muscle Res. Cell Motil.* **13,** 272–284 (1992).
21. Howard, J. *Mechanics of Motor Proteins and the Cytoskeleton* (Sinauer Associates, Inc., Massachusetts, 2001).
22. Murphy, D. B., Gray, R. O., Grasser, W. A. & Pollard, T. D. Direct demonstration of actin filament annealing *in vitro*. *J. Cell Biol.* **106,** 1947–1954 (1988).
23. Brenner, S. L. & Korn, E. D. On the mechanism of actin monomer–polymer subunit exchange at steady state. *J. Biol. Chem.* **258,** 5013–5020 (1983).
24. Spudich, J. A. & Watt, S. The regulation of rabbit skeletal muscle contraction. I. Biochemical studies of the interaction of the tropomyosin–troponin complex with actin and the proteolytic fragments of myosin. *J. Biol. Chem.* **246,** 4866–4871 (1971).
25. Yasuda, R., Miyata, H. & Kinosita, K. Jr. Direct measurement of the torsional rigidity of single actin filaments. *J. Mol. Biol.* **263,** 227–236 (1996).
26. Kouyama, T. & Mihashi, K. Fluorimetry study of *N*-(1-pyrenyl) iodoacetamide-labelled F-actin. Local structural change of actin protomer both on polymerization and on binding of heavy meromyosin. *Eur. J. Biochem.* **114,** 33–38 (1981).
27. Funatsu, T., Harada, Y., Tokunaga, M., Saito, K. & Yanagida, T. Imaging of single fluorescent molecules and individual ATP turnovers by single myosin molecules in aqueous solution. *Nature* **374,** 555–559 (1995).

ACKNOWLEDGEMENTS

This research was partly supported by Grants-in-Aid for Scientific Research, Scientific Research on Priority Areas and Bio-venture Projects from the Ministry of Education, Culture, Sports, Science and Technology of Japan, and by Grants-in-Aid from the Japan Science and Technology Corporation (CREST) and the Mitsubishi Foundation. We thank W. Rozycki for reading the manuscript. We also thank colleagues at Waseda University and CREST for their encouragement and support. I.F. is a research fellow of the Japan Society for the Promotion of Science.
Correspondence and requests for material should be addressed to S.I.

COMPETING FINANCIAL INTERESTS

The authors declare that they have no competing financial interests.